MR1-restricted MAIT cells display ligand discrimination and pathogen selectivity through distinct T cell receptor usage

Marielle C. Gold,[1,2,4] James E. McLaren,[5] Joseph A. Reistetter,[1]
Sue Smyk-Pearson,[1] Kristin Ladell,[5] Gwendolyn M. Swarbrick,[3]
Yik Y.L. Yu,[6] Ted H. Hansen,[6] Ole Lund,[7] Morten Nielsen,[7,8] Bram Gerritsen,[9]
Can Kesmir,[9] John J. Miles,[5,10] Deborah A. Lewinsohn,[2,3] David A. Price,[5,11]
and David M. Lewinsohn[1,2,4]

[1]Division of Pulmonary and Critical Care Medicine, [2]Department of Molecular Microbiology and Immunology,
 and [3]Department of Pediatrics, Oregon Health and Science University, Portland, OR 97239
[4]Portland VA Medical Center, Portland, OR 97239
[5]Institute of Infection and Immunity, Cardiff University School of Medicine, Cardiff CF14 4XN, Wales, UK
[6]Department of Pathology and Immunology, Washington University in St. Louis School of Medicine, St. Louis, MO 63110
[7]Center for Biological Sequence Analysis, Department of Systems Biology, Technical University of Denmark, 2800 Lyngby, Denmark
[8]Instituto de Investigaciones Biotecnológicas, Universidad Nacional de San Martín, 1650 San Martín, Buenos Aires, Argentina
[9]Theoretical Biology and Bioinformatics Group, Utrecht University, 3584 CH Utrecht, Netherlands
[10]QIMR Berghofer Medical Research Institute, Brisbane, Queensland 4006, Australia
[11]Human Immunology Section, Vaccine Research Center, National Institute of Allergy and Infectious Diseases,
 National Institutes of Health, Bethesda, MD 20892

Mucosal–associated invariant T (MAIT) cells express a semi–invariant T cell receptor (TCR) that detects microbial metabolites presented by the nonpolymorphic major histocompatibility complex (MHC)–like molecule MR1. The highly conserved nature of MR1 in conjunction with biased MAIT TCRα chain usage is widely thought to indicate limited ligand presentation and discrimination within a pattern–like recognition system. Here, we evaluated the TCR repertoire of MAIT cells responsive to three classes of microbes. Substantial diversity and heterogeneity were apparent across the functional MAIT cell repertoire as a whole, especially for TCRβ chain sequences. Moreover, different pathogen–specific responses were characterized by distinct TCR usage, both between and within individuals, suggesting that MAIT cell adaptation was a direct consequence of exposure to various exogenous MR1–restricted epitopes. In line with this interpretation, MAIT cell clones with distinct TCRs responded differentially to a riboflavin metabolite. These results suggest that MAIT cells can discriminate between pathogen–derived ligands in a clonotype–dependent manner, providing a basis for adaptive memory via recruitment of specific repertoires shaped by microbial exposure.

CORRESPONDENCE
Marielle C. Gold:
goldm@ohsu.edu
OR
David M. Lewinsohn:
lewinsod@ohsu.edu

Mucosal-associated invariant T (MAIT) cells are characterized by the expression of a semi-invariant TCR that engages antigenic ligands restricted by the nonpolymorphic MHC-like molecule MR1. Human MAIT TCRs typically comprise a *TRAV1-2/TRAJ33* gene–encoded α chain paired with a β chain constructed from *TRBV20-1* or *TRBV6* family gene segments (Porcelli et al., 1993; Tilloy et al., 1999; Reantragoon et al., 2013). In contrast to conventional αβ T cell populations, pathogen-reactive MAIT cells with effector capacity can be found in the human thymus (Gold et al., 2013). Moreover, their selection depends on hematopoietic cells rather than thymic epithelium (Treiner et al., 2005; Martin et al., 2009). Collectively, these attributes suggest that MAIT cells constitute an innate T cell subset with conserved recognition properties.

Despite these innate-like features, several lines of evidence support the hypothesis that pathogen-reactive MAIT cells adapt to their environment.

M.C. Gold and J.E. McLaren contributed equally to this paper.
D.A. Price and D.M. Lewinsohn contributed equally to this paper.

The Journal of Experimental Medicine

The Rockefeller University Press $30.00
J. Exp. Med. 2014 Vol. 211 No. 8   1601–1610
www.jem.org/cgi/doi/10.1084/jem.20140507

1601

Table 1. Summary of TCR usage in human MAIT cell clones

Clone ID	TRBV	TRAJ	CDR3α
D470_B1[a]	20-1	20	CAVNGDDYKLSF
D481_F12	4-2	20	CAVRDSDYKLSF
D481_C7	6-4	20	CAVSLQDYKLSF
D571_A1	6-4	20	CAVRDGDYKLSF
D426_G11	6–4	33	**CAVRDSNYQLIW**
D426_B1[a]	6–4	33	**CAVRDSNYQLIQW**
D466_F5[a]	6–4	33	**CAVRDSNYQLIQW**
D571_A10–2	6–4	33	**CAVRDSNYQLIW**
D481_A9	*20–1*	*33*	*CAAMDSNYQLIW*
D504_F9-2	*20–1*	*33*	*CAAMDSNYQLIW*
D466_A3	20-1	33	CAVLDSNYQLIW
D450_C8[a]	6-2/3	33	CARSDSNYQLIW
D426_A6	6-4	33	CAVMDSNYQLIW
D426_G1	6-5	33	CAVSDSNYQLIW
D470_F6	6-6	33	CAALDSNYQLIW
D504_H11	17	33	CASMDSNYQLIW

Putative TCR families appear in bold and italics.
[a]Previously described in Gold et al. (2010).

It is established that MAIT cells detect a broad range of microorganisms (Gold et al., 2010; Le Bourhis et al., 2010) and contribute to the control of several pathogens in mice, including *Klebsiella pneumoniae* (Georgel et al., 2011), *Francisella tularensis* (Meierovics et al., 2013), and mycobacterial species (Le Bourhis et al., 2010; Chua et al., 2012). Furthermore, MAIT cells expand in the periphery after thymic egress as a consequence of microbial colonization (Martin et al., 2009; Le Bourhis et al., 2010). In line with these observations, human MAIT cells display a naive phenotype in cord blood but acquire characteristics associated with exogenous antigen exposure in adults (Dusseaux et al., 2011; Gold et al., 2013). However, the microbial and environmental signals that lead to the migration, differentiation, expansion, and maintenance of MAIT cells are not understood.

Although the MAIT TCR has been described as semi-invariant, there is sufficient plasticity within the repertoire to allow for the possibility of diverse ligand recognition. Indeed, MAIT TCRs are not exclusively germline-encoded and incorporate sequence variability as a consequence of V(D)J recombination (Tilloy et al., 1999; Greenaway et al., 2013; Reantragoon et al., 2013). This process of somatic gene rearrangement potentially enables pathogen-specific recognition within the confines of restricted TCR gene usage.

Recently, MR1 has been shown to bind small organic compounds derived from microbial vitamin B biosynthetic pathways (Kjer-Nielsen et al., 2012). Although MR1 binds metabolites of vitamin B9 (folic acid), only three derivatives of vitamin B2 (riboflavin), rRL-6-CH2OH, RL-6-Me-7-OH, and RL-6,7-diMe, are known to stimulate MAIT cells (Kjer-Nielsen et al., 2012). Consistent with this observation, microorganisms with the capacity to synthesize riboflavin have been associated with MAIT cell activation (Gold et al., 2010;

Le Bourhis et al., 2010; Kjer-Nielsen et al., 2012). However, structural studies have revealed that MR1 is promiscuous in its ability to bind and present diverse ligands (Reantragoon et al., 2012; López-Sagaseta et al., 2013a; Patel et al., 2013). Accordingly, there may be discrete pathogen-associated ligands that are yet to be identified.

In this study, we evaluated the ex vivo TCR repertoire of pathogen-reactive MAIT cells responsive to *Mycobacterium smegmatis*, *Salmonella typhimurium*, and *Candida albicans*. Clonotype usage was complex and highly selective within individuals, suggesting a diverse array of MR1-restricted microbial ligands. Moreover, different pathogen-specific responses were characterized by distinct TCR repertoires, both between and within individuals. Direct evidence of MR1-restricted ligand discrimination at the clonal level further supported the potential for unique patterns of pathogen recognition by MAIT cells. Collectively, these data provide a basis for specific TCR repertoire mobilization within an innate-like system shaped by previous microbial exposure.

RESULTS

The TCR repertoire of MAIT cells identified using an MR1 tetramer loaded with the stimulatory vitamin B metabolite, rRL-6-CH2OH, was recently shown to be more heterogeneous than expected based on previous studies (Reantragoon et al., 2013). Moreover, MAIT cells can detect infection with a wide range of bacteria and fungi (Gold et al., 2010; Le Bourhis et al., 2010), which likely have diverse metabolic pathways. In this context, we aimed to determine the relationship between TCR usage and pathogen discrimination.

In earlier work, we used limiting dilution analysis to generate a panel of *Mycobacterium tuberculosis* (Mtb)–reactive CD8^{+} MAIT cell clones (Gold et al., 2010). All of these clones expressed TRAV1-2^{+} TCRs and recognized Mtb-infected cells in an MR1-restricted manner as determined by Vα7.2-specific mAb staining and functional blockade with an αMR1 mAb, respectively (not depicted; Gold et al., 2010). Sequence analysis confirmed this finding and further revealed that the majority of clones also incorporated the canonical *TRAJ33* gene segment (Table 1). However, 4/16 clones expressed TRAJ20 (Gold et al., 2010), suggesting that pathogen-reactive MAIT cells could yield additional TCR specificities. Moreover, we observed that MAIT cells from different individuals segregated into TCR families through preferential pairing of specific TCRα and TCRβ chains (Table 1). For example, clones A9 and F9-2 from donors 481 and 504, respectively, expressed identical TRAV1-2/TRAJ33^{+} α chains paired with TRBV20-1[+] β chains.
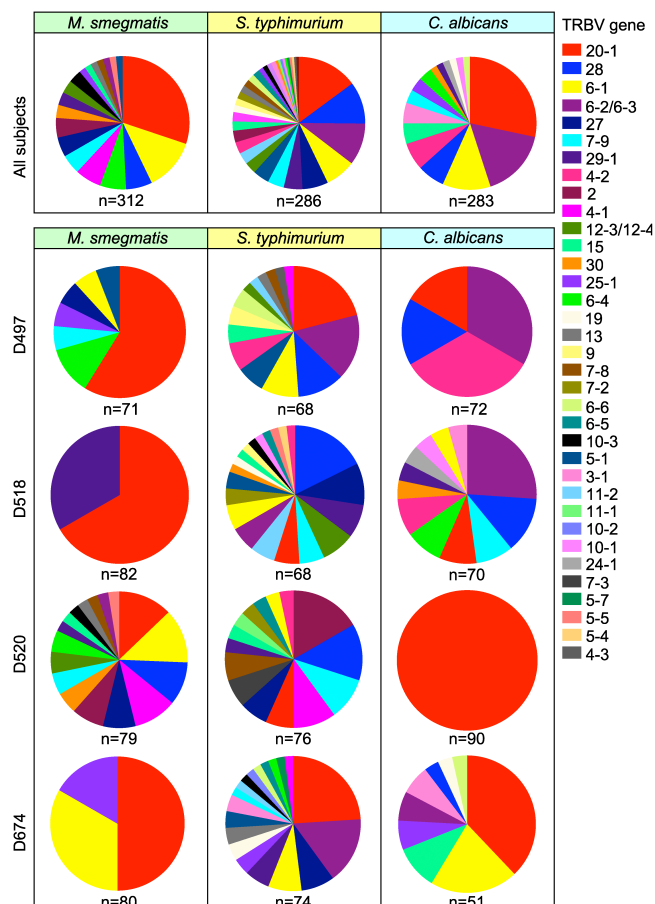
To extend these findings beyond the Mtb-specific setting, we used an unbiased molecular approach to evaluate the MAIT TCR repertoire across diverse bacterial and fungal species. Peripheral blood CD8^{+} T cells from four unrelated adult donors were stimulated directly ex vivo by exposure to A549 epithelial cells infected with *M. smegmatis*, *S. typhimurium*, or *C. albicans* to identify pathogen-reactive MAIT cells restricted by MR1 (Gold et al., 2010, 2013). Functionally responsive MAIT
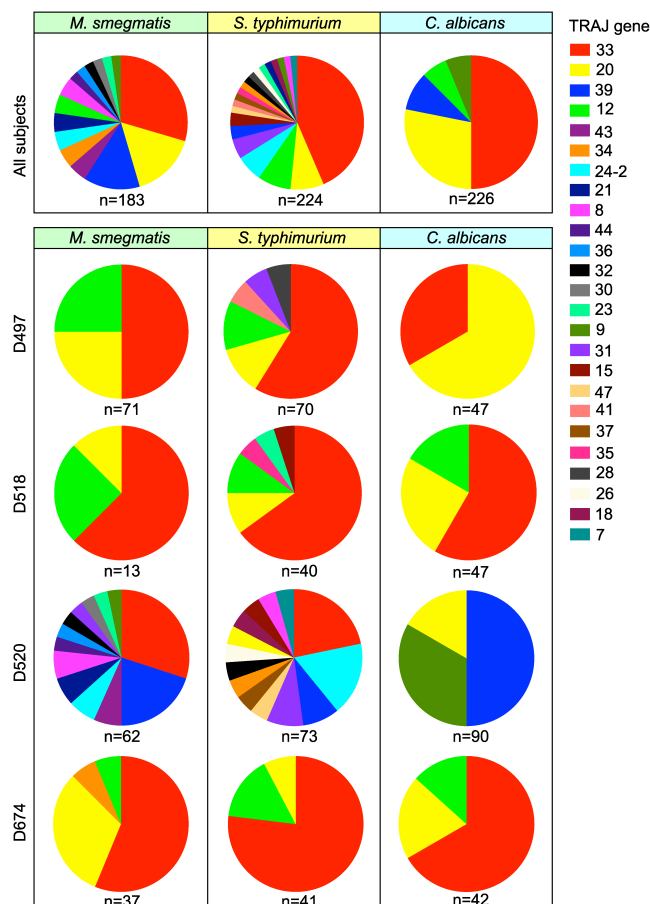
Figure 1. Pathogen–reactive MAIT TCRα chains are not confined to TRAV1–2/TRAJ33 rearrangements. Human CD8+ MAIT cells from four individuals were stimulated overnight using A549 cells infected with *M. smegmatis*, *S. typhimurium*, or *C. albicans*. Live, pathogen-reactive MAIT cells were then isolated by flow cytometry based on coexpression of TRAV1-2 and TNF. Unbiased molecular analysis of expressed *TRA* gene products was performed as described in Materials and methods. Aggregate *TRAJ* gene profiles from all four donors in response to each pathogen ($n = 3$) are shown at the top; data from individual donors are shown underneath as indicated. Each sequence was counted once regardless of frequency. Total sequence counts are indicated in each case.

Figure 2. Pathogen–reactive MAIT TCRβ chains are diverse. Details as described in the legend to Fig. 1, except that *TRBV* gene usage was analyzed. Aggregate *TRBV* gene profiles from all four donors in response to each pathogen ($n = 3$) are shown at the top; data from individual donors are shown underneath as indicated. Each sequence was counted once regardless of frequency. Total sequence counts are indicated in each case.

cells were isolated for repertoire experiments at high purity using a flow cytometric sorting strategy to detect viable TRAV1-2+ cells expressing TNF (Haney et al., 2011). Response sizes varied from 0.5 to 6.9% of the TRAV1-2+ CD8+ T cell population with no significant differences between pathogens. Clonotypic analysis was then performed using a template switch–anchored RT-PCR as described previously (Quigley et al., 2011).

An aggregated analysis of *TRAJ* gene usage by pathogen-reactive TRAV1-2+ MAIT TCRs is shown in Fig. 1. Although the canonical TRAV1-2/TRAJ33 rearrangement dominated the TCRα chain repertoire, alternative *TRAJ* genes were commonly used. In particular, substantial proportions of the TRAV1-2/non-TRAJ33 rearrangements incorporated TRAJ20 or TRAJ12 segments. Moreover, an array of *TRAJ* genes not previously known to associate with pathogen–reactive, TRAV1-2+ MAIT cells were

identified. Of these noncanonical genes, *TRAJ9* and *TRAJ39* do not encode the Tyr95α residue present in TRAJ33, TRAJ20, and TRAJ12 (Reantragoon et al., 2013), which is thought to be critical for MAIT cell activation (Reantragoon et al., 2012; Patel et al., 2013; Young et al., 2013). Due to the lack of allelic exclusion at the *TRA* locus, however, we cannot definitively assign these α chains to functional heterodimeric TCRs.

Notable differences in *TRAJ* gene usage were apparent across pathogen-reactive MAIT cell populations. In terms of overall distribution, diversity was greatest for *S. typhimurium* and most restricted for *C. albicans*. Individual *TRAJ* gene usage also differed across specificities within each individual. This was most striking in donor 520 (D520). Here, *TRAV1-2/TRAJ33* gene–encoded TCRs were elicited in response to *M. smegmatis* and *S. typhimurium*, but not in response to *C. albicans*. Collectively, these data demonstrate that pathogen–reactive TRAV1-2+ MAIT cells can productively incorporate a broad array of *TRAJ* gene segments with differential usage across pathogen specificities.
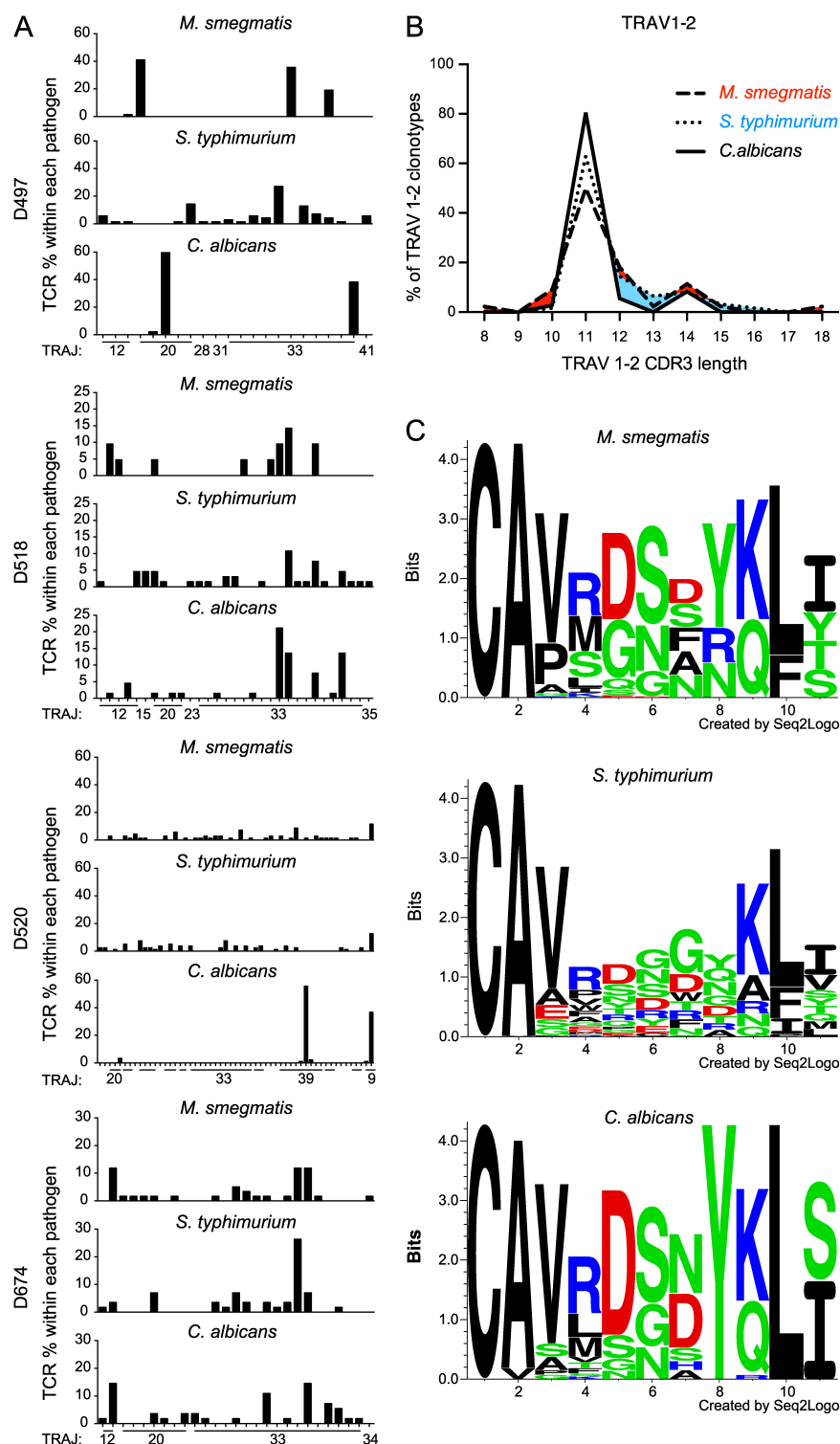
Figure 3. MAIT TRAV1–2+ CDR3α sequences display length and sequence similarity. (A) Representation of unique TRAV1-2+ CDR3α sequences from each donor in response to each pathogen as indicated. Each bar represents a distinct sequence, the relative frequency of which is depicted on the y axis. *TRAJ* gene usage is shown on the x axis labeled for dominant sequences. (B) Distribution of CDR3α amino acid lengths from TRAV1-2+ MAIT cells responsive to each pathogen as indicated in the key. (C) Visual representation of amino acid enrichments at each position across the CDR3α core compiled from pathogen-reactive MAIT cell TRAV1-2+ sequences. Analysis was confined to CDR3α sequences with a length of 11 amino acids, encompassing 39 sequences for *M. smegmatis*, 61 for *S. typhimurium*, and 30 for *C. albicans*. Graphics were generated using Seq2Logo.

A similar analysis is shown for *TRBV* gene usage in Fig. 2. Across the dataset as a whole, 35 different *TRBV* genes were represented within the pathogen–reactive MAIT cell repertoire. Most frequent among these were the *TRBV20-1* and *TRBV6* family gene members. In contrast, these *TRBV* genes were used by <6% of nonresponsive TRAV1-2+ cells, which expressed a diverse array of *TRBV* genes without apparent enrichments (not depicted). As above, *TRBV* gene usage was most diverse for *S. typhimurium* and varied across specificities within each individual. In D520, for example, the MAIT cell response to *C. albicans* was composed entirely of TRBV20-1+ TCRs, yet these were relatively rare in the corresponding responses

to *S. typhimurium* and *M. smegmatis*. Thus, MAIT cells use diverse *TRBV* gene segments with variable clonotypic deployment across pathogen specificities.

Previous studies have demonstrated that MAIT TCRα chains are not exclusively germline encoded (Tilloy et al., 1999; Treiner et al., 2005; Gold et al., 2010; Goldfinch et al., 2010) and most often contain single nucleotide additions that contribute to CDR3 core diversity (Greenaway et al., 2013). We therefore performed an in-depth analysis of CDR3α sequences across our dataset (Fig. 3).

Unique CDR3α sequences within the TRAV1-2⁺ repertoire are displayed across donors and specificities in Fig. 3 A. In these graphics, each bar represents a distinct sequence plotted as a function of *TRAJ* gene usage (x axis) and relative frequency (y axis). Disparate patterns were observed, suggesting pathogen-specific MAIT cell reactivity. In D497, for example, *M. smegmatis* and *C. albicans* elicited three predominant TRAV1-2⁺ sequences that were distinct from one another; a broader repertoire was activated in response to *S. typhimurium*, which again differed at the level of CDR3α sequence usage. Similarly, the TRAV1-2⁺ MAIT cell response to *C. albicans* was dominated by two unique sequences in D520, whereas broader repertoires were elicited by *M. smegmatis* and *S. typhimurium*. Thus, the MAIT cell response to each of these microbes was characterized by unique TCRα usage within individuals.

Although no unique TRAV1-2⁺ sequence appeared to associate with a single pathogen or a single donor, we wanted to evaluate patterns of amino acid usage across pathogen specificities. To perform this analysis on the greatest number of TRAV1-2⁺ transcripts, we selected CDR3α sequences containing 11 amino acid residues (Fig. 3 B). This subset contained 39 sequences for *M. smegmatis*, 61 for *S. typhimurium*, and 30 for *C. albicans*. Representative logos highlighting preferential amino acid usage for each pathogen are shown in Fig. 3 C. Particular amino acid motifs were prevalent within the TRAV1-2⁺ sequences for each pathogen. For example, tyrosine (Y) was highly prevalent at position 8 in *C. albicans*–reactive MAIT cells, whereas glycine (G) was favored at position 7 for *S. typhimurium*. To quantify this observation further, we compared the similarity of TRAV1-2⁺ sequences within a given group, defined by donor or pathogen, to the corresponding sequence similarity between groups (Shen et al., 2012). The analysis across donors shown in Table 2 (A) demonstrates two points. First, overall similarity is high, given that a value of 1 represents 100% similarity. Second, similarity within each donor is consistently greater than the similarity between donors. Similar patterns were observed across pathogen specificities (Table 2, B). The significance of these analyses was evaluated using an exact permutation test. Here, each observed TRAV1-2⁺ sequence was randomly assigned to a donor-pathogen pair to determine whether such associations could lead to a result where the similarity within donors and pathogens (intrasimilarity) was consistently higher than the similarity between donors and pathogens (intersimilarity). None of the permutations across 1,000 rounds resulted in higher intersimilarity (P < 0.001). Collectively, these data suggest that MAIT TCR

Table 2. Similarity analyses of TRAV1-2⁺ CDR3 sequences

Group 1	Group 2	Similarity
(A) Similarity analysis across individuals		
D497	D497	**0.947**
D497	D518	0.940
D497	D520	0.935
D497	D674	0.942
D518	D497	0.899
D518	D518	**0.912**
D518	D520	0.901
D518	D674	0.905
D520	D497	0.858
D520	D518	0.866
D520	D520	**0.903**
D520	D674	0.861
D674	D497	0.906
D674	D518	0.913
D674	D520	0.907
D674	D674	**0.923**
(B) Similarity analyses across pathogens		
C. albicans	*C. albicans*	**0.934**
C. albicans	*S. typhimurium*	0.925
C. albicans	*M. smegmatis*	0.927
S. typhimurium	*C. albicans*	0.896
S. typhimurium	*S. typhimurium*	**0.906**
S. typhimurium	*M. smegmatis*	0.902
M. smegmatis	*C. albicans*	0.901
M. smegmatis	*S. typhimurium*	0.910
M. smegmatis	*M. smegmatis*	**0.916**

Bolded values denote those with the highest similarity within each comparison group.

chains can discriminate between ligands. Although we have no knowledge of each individual's microbial exposure history, the repertoire observed for any particular microbial pathogen may reflect prior ligand exposure. At present, the precise nature of such MR1-restricted antigens and their relationship to TCR usage remains unknown.

To assess true clonotypic diversity, we similarly evaluated TCRβ chain usage across donors and specificities (Fig. 4). For this purpose, we selected TRBV20-1⁺ sequences, which represent the most common *TRBV* gene–defined clonotypes across pathogen-reactive MAIT cells. As above, unique TRBV20-1⁺ sequences were associated with each pathogen specificity. In D497, for example, MAIT cell populations specific for *S. typhimurium* and *C. albicans* incorporated different CDR3β loops despite equivalent *TRBV20-1* gene usage (Fig. 4 A); these sequences were further distinct from those responsive to *M. smegmatis* (Fig. 4 A). Similar findings applied to other *TRBV* gene families (not depicted). Moreover, across the entire dataset, only four shared TCRβ clonotypes were detected between donors; notably, each of these sequences was associated with more than one pathogen specificity (not depicted). Thus, in sharp contrast to the TCRα chain repertoire, minimal TCRβ overlap was present across donors and pathogens.
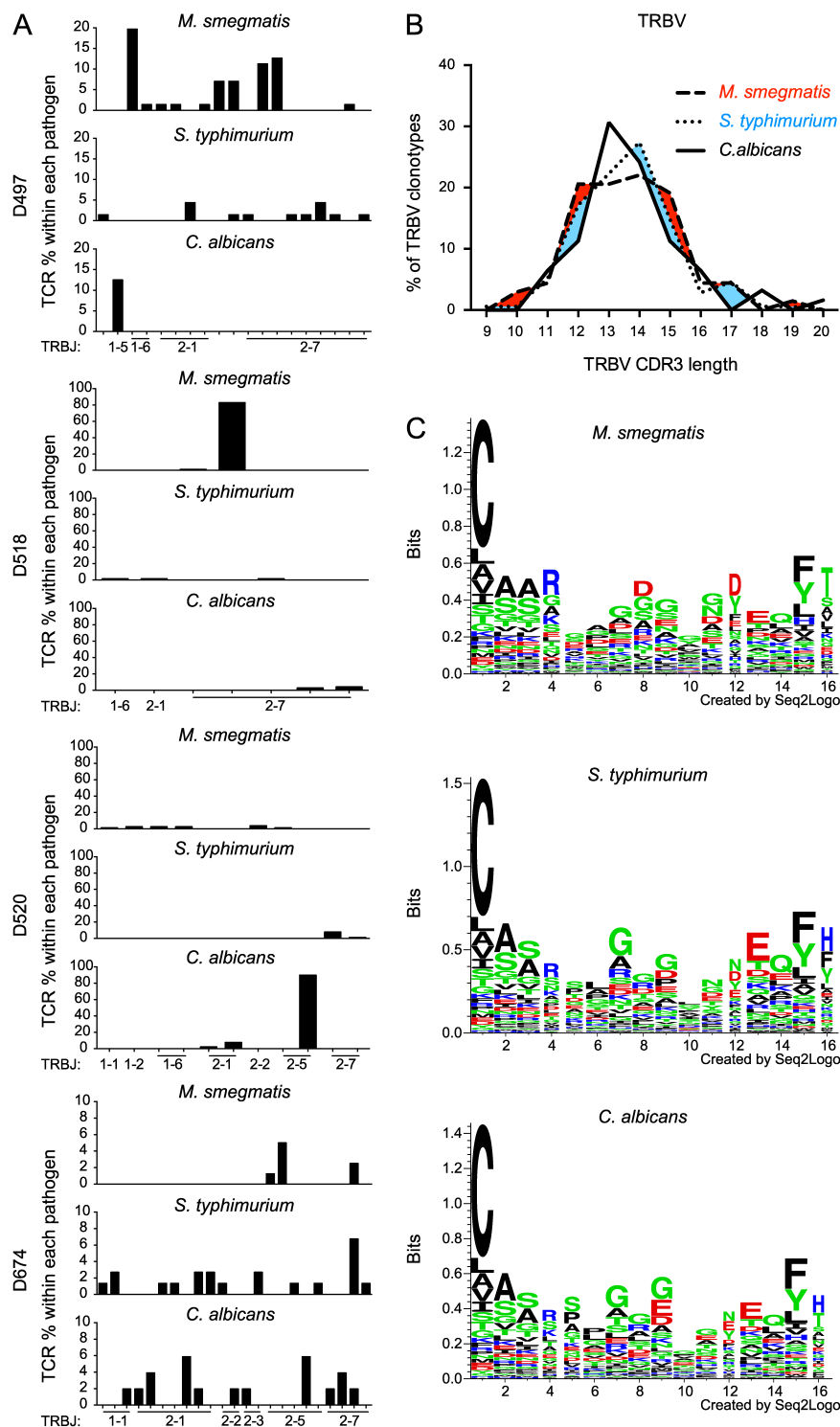
Figure 4. MAIT CDR3β usage is unique across individuals and pathogens. (A) Representation of unique TRBV20-1+ CDR3β sequences from each donor in response to each pathogen as indicated. Each bar represents a distinct sequence, the relative frequency of which is depicted on the y axis. *TRBJ* gene usage is shown on the x axis labeled for dominant sequences. (B) Distribution of CDR3β amino acid lengths from all *TRBV* gene–defined MAIT cells responsive to each pathogen as indicated in the key. (C) Visual representation of amino acid enrichments at each position across the CDR3β core compiled from pathogen-reactive MAIT cell TRBV+ sequences. Analysis was confined to CDR3β sequences with a length of 13 or 14 amino acids, encompassing 34 sequences for *M. smegmatis*, 75 for *S. typhimurium*, and 39 for *C. albicans*. Graphics were generated using Seq2Logo.

To evaluate amino acid usage across specificities, we selected all clonotypes with CDR3β sequences containing 13 or 14 residues, based on prevalence within the length distribution profile (Fig. 4 B). This subset contained 34 sequences for *M. smegmatis*, 75 for *S. typhimurium*, and 39 for *C. albicans*. No obvious motifs were present across the CDR3β core, although

TRBJ gene–encoded phenylalanine (F) and tyrosine (Y) residues were notably represented at the C terminus, potentially reflecting amino acid conservation linked to preferential usage of TRBJ1-1, TRBJ2-1, and TRBJ2-7 (Fig. 4 C). To extend these observations, we performed similarity analyses for the most common *TRBV* gene–defined clonotypes in our dataset

(*TRBV20-1*, *TRBV6-1*, *TRBV6-2/3*, and *TRBV28*), comprising a total of 148 unique sequences across all donors and pathogens (Table 3, A and B). Again, the similarity indices were consistently high, but nevertheless lower than for the TRAV1-2$^+$ sequences, reflecting a more diverse TCRβ repertoire. Furthermore, intrasimilarity was significantly greater than intersimilarity for all *TRBV* gene–defined comparison groups across donors (Table 3, A) and pathogens (Table 3, B). This latter observation is particularly remarkable in the case of *S. typhimurium*, which mobilized a highly diverse set of TCRβ clonotypes (median Simpson's diversity index, 0.934–0.983) compared with *M. smegmatis* and *C. albicans* (median Simpson's diversity index, 0.221/0.184 to 0.971/0.966, respectively). Finally, we compared the similarity of *TRBV* gene–defined sequences in TRAV1-2$^+$ nonreactive (TNF$^-$) cells isolated during the *C. albicans* stimulation protocol with the corresponding pathogen-reactive (TNF$^+$) populations. The greatest level of similarity was observed among the nonreactive TRAV1-2$^+$ cells (Table 3, C). Collectively, these analyses support the conclusion that different pathogen-associated antigens drive distinct donor-specific TCRβ clonotype expansions within the MAIT cell population.

To confirm this hypothesis, we tested four TCR–distinct MAIT cell clones (Table 1; Gold et al., 2010) for reactivity against the riboflavin-derived MR1-restricted ligand RL-6,7-diMe (Kjer–Nielsen et al., 2012) in IFN-γ ELISPOT assays. Only two clones recognized RL-6,7-diMe (Fig. 5 A), even though all four were comparably stimulated by presenting cells infected with *M. smegmatis*. The stronger agonist rRL-6-CH$_2$OH was not tested (Kjer–Nielsen et al., 2012; Corbett et al., 2014). Moreover, each clone responded similarly to each of the three pathogens used for TCR analysis (Fig. 5 B). Notably, all four clones contain the Tyr95α residue thought to be essential for MR1-restricted recognition (Reantragoon et al., 2012; Patel et al., 2013; Young et al., 2013). Nevertheless, this characteristic in isolation was not sufficient for universal activation by RL-6,7-diMe. Thus, MAIT cells can discriminate between MR1-restricted ligands.

DISCUSSION

In this study, we evaluated the ex vivo TCR repertoire of MAIT cells responsive to three distinct classes of pathogens. Substantial diversity and heterogeneity were apparent across the functional MAIT cell repertoire as a whole, especially for TCRβ chain sequences. Moreover, different pathogen-specific responses were characterized by distinct TCR usage, both between and within individuals, suggesting that MAIT cell adaptation was a direct consequence of exposure to various exogenous MR1-restricted epitopes. In line with this interpretation, MAIT cell clones with distinct TCRs responded differentially to a riboflavin metabolite. These results suggest that MAIT cells can discriminate between pathogen-derived ligands in a clonotype-dependent manner, potentially enabling adaptive memory within a pattern-like recognition system.

MAIT cells were originally defined by the expression of a canonical semi-invariant TRAV1-2/TRAJ33 TCRα chain

Table 3. Similarity analyses of TRBV6-1$^+$, TRBV6-2/3$^+$, TRBV20-1$^+$, and TRBV28$^+$ CDR3 sequences

Group 1	Group 2	Similarity
(A) Similarity analyses across individuals		
D497	D497	**0.858**
D497	D518	0.840
D497	D520	0.838
D497	D674	0.852
D518	D497	0.852
D518	D518	**0.859**
D518	D520	0.838
D518	D674	0.849
D520	D497	0.841
D520	D518	0.830
D520	D520	**0.850**
D520	D674	0.837
D674	D497	0.849
D674	D518	0.837
D674	D520	0.833
D674	D674	**0.858**
(B) Similarity analyses across pathogens		
C. albicans	*C. albicans*	**0.861**
C. albicans	*S. typhimurium*	0.855
C. albicans	*M. smegmatis*	0.842
C. albicans	TRAV1-2$^+$ TNF$^-$	0.853
S. typhimurium	*C. albicans*	0.842
S. typhimurium	*S. typhimurium*	**0.855**
S. typhimurium	*M. smegmatis*	0.838
S. typhimurium	TRAV1-2$^+$ TNF$^-$	0.847
M. smegmatis	*C. albicans*	0.843
M. smegmatis	*S. typhimurium*	0.853
M. smegmatis	*M. smegmatis*	**0.869**
M. smegmatis	TRAV1-2$^+$ TNF$^-$	0.848
(C) Similarity analyses across nonreactive (TNF$^-$) and pathogen–reactive (TNF$^+$) subsets		
TRAV1-2$^+$ TNF$^-$	*M. smegmatis*	0.844
TRAV1-2$^+$ TNF$^-$	*S. typhimurium*	0.857
TRAV1-2$^+$ TNF$^-$	*C. albicans*	0.845
TRAV1-2$^+$ TNF$^-$	TRAV1-2$^+$ TNF$^-$	**0.858**

Bolded values denote those with the highest similarity within each comparison group.

(Porcelli et al., 1993; Tilloy et al., 1999). Additional TCRα complexity was subsequently demonstrated in Mtb-reactive MAIT cell clones (Gold et al., 2010) and more recently in rRL-6-CH$_2$OH/MR1 tetramer–reactive cells (Reantragoon et al., 2013). In line with the latter study, pathogen-reactive MAIT cells frequently expressed *TRAJ33*, *TRAJ12*, and *TRAJ20* gene transcripts. Each of these genes encodes the Tyr95α residue thought to be essential for MR1-restricted ligand recognition (Reantragoon et al., 2012; López–Sagaseta et al., 2013a; Patel et al., 2013). Our study identifies two additional *TRAJ* genes, namely *TRAJ41* and *TRAJ28*, which also encode Tyr95α in MAIT cells. Further *TRAJ* gene transcripts,
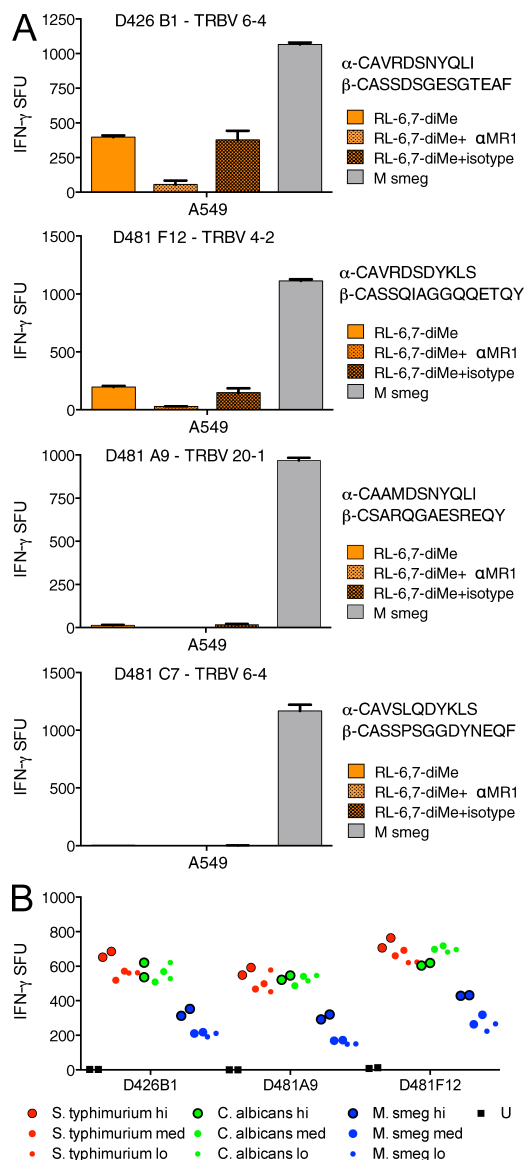
Figure 5. MR1–restricted MAIT cell clones display ligand discrimi–nation for the vitamin B metabolite RL–6,7–diMe. (A) A549 cells (20,000 per well) were pulsed with 5 μg/ml RL-6,7-diMe overnight and tested for their ability to stimulate MR1-restricted clones (10,000 per well) in IFN-γ ELISPOT assays. Clones D426 B1 and D481 A9 express TRAJ33; clones D481 F12 and D481 C7 express TRAJ20. TRBV usage and CDR3α and CDR3β sequences are indicated. Error bars represent SEM of duplicate determinations. (B) A549 cells (25,000 per well) were infected with *S. typhimurium*, *C. albicans*, or *M. smegmatis* at an MOI of 50 (hi), 25 (med), or 12.5 (lo) and then incubated overnight with the indicated MR1-restricted MAIT cell clones (10,000 per well) in duplicate wells. IFN-γ pro-duction was quantified by ELISPOT. Similar results were obtained from a minimum of three independent experiments.

such as *TRAJ9* and *TRAJ39*, were detected that do not en-code Tyr95α. In one donor (D520), these two genes domi-nated TRAJ usage in MAIT cells responsive to *C. albicans*, but not *M. smegmatis* or *S. typhimurium*, suggesting alternative modes of TCRα engagement. However, the lack of allelic exclusion

at the *TRA* locus precludes definitive conclusions. Nonethe-less, the TCRα repertoire of MAIT cells is clearly more di-verse than previously described and shows features consistent with pathogen selectivity.

Historically, MAIT cells have been associated with *TRBV20-1* and *TRBV6* family genes (Porcelli et al., 1993; Tilloy et al., 1999). More recently, ∼75% of tetramer-reactive MAIT cells were found to express these *TRBV* genes despite the presence of additional heterogeneity (Reantragoon et al., 2013). Although pathogen-reactive MAIT cells frequently displayed *TRBV20-1* and *TRBV6* family gene usage in our study, >50% of all *TRBV* family genes were also detected, re-vealing greater heterogeneity than observed previously. These findings could indicate promiscuous pairing or the potential for diverse ligand recognition mediated by the TCRβ chain. The extent to which the TCRVβ domain contributes to li-gand discrimination remains unclear. Mutagenesis of specific residues in the CDR3β loop did not alter MAIT hybridoma cell recognition of MR1-overexpressing cells loaded with *Sal-monella* supernatants; however, TCRVβ chain swapping abro-gated recognition by the same hybridoma (Reantragoon et al., 2012). These data suggest that the TCRVβ domain contrib-utes to MR1-restricted ligand recognition in ways that remain to be defined. At present, our ex vivo analysis of pathogen-reactive MAIT cells precludes the assignment of αβ pairing. Nonetheless, limited analysis of Mtb-reactive clones points to segregation of MAIT cells into TCR families through prefer-ential pairing of specific TCRα and TCRβ chains. For ex-ample, MAIT cell clones with identical CDR3α chains isolated from different individuals tended to associate with the same *TRBV* gene family. Such putative TCR families may, at least in theory, contribute to greater affinities for spe-cific classes of antigen. Indeed, the observation that only four TCRβ sequences were shared across our entire dataset sug-gests that clonotypic expansions occur in a manner similar to conventional T cells. Accordingly, the observation of unique *TRBV* gene usage across pathogens suggests that TCRβ chains contribute to ligand detection. This conclusion is sup-ported by molecular analyses of MAIT TCR engagement with MR1-presented ligands (Reantragoon et al., 2012; López-Sagaseta et al., 2013a,b; Patel et al., 2013; Young et al., 2013), which have revealed a docking mode similar to that of classical MHC-restricted αβ TCRs and unlike that used by CD1-restricted iNKT cells (Reantragoon et al., 2012; López-Sagaseta et al., 2013a,b; Patel et al., 2013). In this case, the less variable TCRα chain primarily mediates contacts with the MR1 protein, whereas the CDR3β loop is positioned above the MR1 ligand–binding groove. As suggested previously (López-Sagaseta et al., 2013a,b), this topography lends itself to the interpretation that the CDR3β loop can contribute to ligand discrimination.

Based on our findings, we postulate that MR1–restricted ligand diversity drives MAIT cell adaptation and TCR reper-toire diversity. Although not yet described, we presume that the naive MAIT thymocyte population contains a diverse and un-focused precursor repertoire. Subsequently, skewed clonotypic

responses to different pathogens emerge in the periphery as a result of antigenic exposure to a diverse array of MR1-restricted ligands. We further propose that these expansions will reflect distinct microbial challenges. This scenario of differential agonist encounter would explain the unique clonotypic expansions across individuals with different microbial exposure histories. In line with this hypothesis, increased MAIT TCR engagement through the CDR3β loop was recently associated with greater MR1-restricted ligand potency (López-Sagaseta et al., 2013b; Patel et al., 2013). Thus, patterns of clonotypic expansion are likely to reflect high-affinity TCR interactions with distinct MR1 ligands, consistent with previous observations in conventional systems (Price et al., 2005).

Although the possibility exists that stimulatory microorganisms express the same few MR1-restricted riboflavin ligands in different proportions, elegant molecular analyses provide evidence that MR1 can accommodate a range of different ligands (Reantragoon et al., 2012; López-Sagaseta et al., 2013a; Patel et al., 2013). To date, only three MAIT cell epitopes have been identified, all of which are riboflavin metabolites (Kjer-Nielsen et al., 2012; Reantragoon et al., 2012, 2013; Patel et al., 2013). Nonetheless, these antigens share many chemical properties with other microbial and mammalian compounds. It is therefore highly feasible that other MR1-restricted ligands are generated similarly, enabling MAIT cell adaptation to a wide range of microorganisms and their associated metabolomes.

Pathogen-reactive MAIT cells share many features traditionally thought to be associated with both innate and adaptive T cells. Restriction by a nonpolymorphic MHC-like molecule, expression of a semi-invariant TCR, thymically acquired effector function, and intrathymic selection by hematopoietic cells are all considered features of innate T cells. However, after thymic egress, MAIT cells expand and acquire an effector phenotype associated with antigenic exposure. Furthermore, the development of MAIT cells requires the presence of bacteria, suggesting the capacity to adapt in response to environmental signals. Our data provide evidence that MAIT cells can detect a diverse array of MR1-restricted ligands and differentiate selectively in response to specific pathogens akin to classically restricted T cells. Thus, the MAIT TCR enables adaptive immune responses within the confines of a pattern-like recognition system that can discriminate between microorganisms.

MATERIALS AND METHODS

Human subjects. All samples were collected under protocols approved by the Institutional Review Board at Oregon Health and Science University. PBMCs were obtained by apheresis from healthy adult donors with informed consent. Subjects lacked any detectable responses to the immunodominant Mtb antigens CFP-10 and ESAT-6 and were considered unexposed. Exposure to *M. smegmatis*, *S. typhimurium*, and *C. albicans* was not evaluated.

Cells and reagents. A549 cells (ATCC CCL-185) were used as stimulators for direct ex vivo determination of Mtb-reactive T cells. Mtb-specific MAIT cell clones were generated, maintained, and tested by IFN-γ ELISPOT as described previously (Gold et al., 2010). All of these clones expressed TRAV1-2$^+$ TCRs and recognized pathogen-infected cells in an MR1-restricted manner. RL-6,7-diMe was purchased from WuXi AppTec.

Microorganisms and infection of A549 cells. Adherent A549 cells were infected overnight with *M. smegmatis* (multiplicity of infection [MOI] 10), and nonadherent A549 cells were infected for 1 h with *S. typhimurium* (MOI 30) or *C. albicans* (MOI 3) at 37°C. All infections were performed in the absence of antibiotics.

Stimulation and isolation of pathogen-reactive MAIT cells. CD8$^+$ T cells were enriched from PBMCs by negative selection using magnetic bead separation according to the manufacturer's instructions (STEMCELL Technologies), added to uninfected or infected A549 cells at a ratio of 3:1, and incubated for 16 h in the presence of α-TNF (Beckman Coulter) and TAPI-O (EMD Millipore) to prevent TNF cleavage from the cell surface (Haney et al., 2011). The following day, cells were stained with: (a) α-CD4 and α-CD8 (BioLegend) and (b) α-TRAV1-2 and α-TCRγδ (Thermo Fisher Scientific). Dead cells were excluded from the analysis using propidium iodide (BioLegend). Viable CD4$^-$TCRγδ$^-$CD8$^+$TRAV1-2$^+$TNF$^+$ cells were sorted at high purity using a FACSAria flow cytometer (BD) directly into RNAlater (Applied Biosystems). The corresponding nonfunctional populations were sorted in parallel for control purposes. In all cases, cell numbers were standardized (5,000 per aliquot) to minimize sampling bias.

Molecular analysis of TCR usage. Clonotypic analysis of sorted cell populations was performed as described previously (Quigley et al., 2011). In brief, unbiased amplification of all expressed *TRB* or *TRA* gene products was conducted using a template switch–anchored RT-PCR with chain-specific constant region primers. Amplicons were subcloned, sampled, sequenced, and analyzed as described previously (Price et al., 2005). The IMGT nomenclature is used in this study (Lefranc et al., 2003).

Construction of sequence logos. Sequence logos were generated in Shannon format without the use of pseudo counts via the Seq2Logo webserver (Thomsen and Nielsen, 2012). Shannon sequence logos give a visual representation of amino acid enrichments at different positions in the observed CDR3 sequences. The different amino acids are colored according to physicochemical properties (acidic [DE], red; basic [HKR], blue; hydrophobic [ACFILMPVW], black; and neutral [GNQSTY], green). For TRAV1-2, only sequences with a length of 11 amino acids were included (39 sequences for *M. smegmatis*, 61 for *S. typhimurium*, and 30 for *C. albicans*). For TRBV, only sequences with a length of 13 or 14 amino acids were included (34 sequences for *M. smegmatis*, 75 for *S. typhimurium*, and 39 for *C. albicans*). The TRBV sequences were aligned using ClustalX (Larkin et al., 2007) with default parameters set before logo generation. The width of each bar in the sequence logo corresponds inversely with gap density at the given positions.

CDR3 sequence similarity. Similarity between CDR3 sequences was calculated as described previously (Shen et al., 2012). This method allows similarities to be assigned between sequences of different length in an alignment-free manner. In this similarity measure, a perfect match has a similarity score of 1, and a perfect mismatch has a similarity score of 0. To calculate the similarity between two groups of sequences, each sequence from the first group was assigned a score corresponding to the best match against all sequences from the other group (excluding identical matches), and the similarity between the two groups was calculated as the mean of these similarity measures over all sequences within the first group.

CDR3 sequence diversity. Simpson's diversity index was calculated using the randomization method as described previously (Venturi et al., 2007). The median value for each population was derived from 10,000 random draws standardized to the lowest sample size.

REFERENCES

Chua, W.J., S.M. Truscott, C.S. Eickhoff, A. Blazevic, D.F. Hoft, and T.H. Hansen. 2012. Polyclonal mucosa-associated invariant T cells have unique innate functions in bacterial infection. *Infect. Immun.* 80:3256–3267. http://dx.doi.org/10.1128/IAI.00279-12

Corbett, A.J., S.B. Eckle, R.W. Birkinshaw, L. Liu, O. Patel, J. Mahony, Z. Chen, R. Reantragoon, B. Meehan, H. Cao, et al. 2014. T-cell activation by transitory neo-antigens derived from distinct microbial pathways. *Nature.* 509:361–365. http://dx.doi.org/10.1038/nature13160

Dusseaux, M., E. Martin, N. Serriari, I. Péguillet, V. Premel, D. Louis, M. Milder, L. Le Bourhis, C. Soudais, E. Treiner, and O. Lantz. 2011. Human MAIT cells are xenobiotic-resistant, tissue-targeted, CD161hi IL-17–secreting T cells. *Blood.* 117:1250–1259. http://dx.doi.org/10.1182/blood-2010-08-303339

Georgel, P., M. Radosavljevic, C. Macquin, and S. Bahram. 2011. The non-conventional MHC class I MR1 molecule controls infection by *Klebsiella pneumoniae* in mice. *Mol. Immunol.* 48:769–775. http://dx.doi.org/10.1016/j.molimm.2010.12.002

Gold, M.C., S. Cerri, S. Smyk-Pearson, M.E. Cansler, T.M. Vogt, J. Delepine, E. Winata, G.M. Swarbrick, W.-J. Chua, Y.Y.L. Yu, et al. 2010. Human mucosal associated invariant T cells detect bacterially infected cells. *PLoS Biol.* 8:e1000407. http://dx.doi.org/10.1371/journal.pbio.1000407

Gold, M.C., T. Eid, S. Smyk-Pearson, Y. Eberling, G.M. Swarbrick, S.M. Langley, P.R. Streeter, D.A. Lewinsohn, and D.M. Lewinsohn. 2013. Human thymic MR1-restricted MAIT cells are innate pathogen-reactive effectors that adapt following thymic egress. *Mucosal Immunol.* 6:35–44. http://dx.doi.org/10.1038/mi.2012.45

Goldfinch, N., P. Reinink, T. Connelley, A. Koets, I. Morrison, and I. Van Rhijn. 2010. Conservation of mucosal associated invariant T (MAIT) cells and the MR1 restriction element in ruminants, and abundance of MAIT cells in spleen. *Vet. Res.* 41:62. http://dx.doi.org/10.1051/vetres/2010034

Greenaway, H.Y., B. Ng, D.A. Price, D.C. Douek, M.P. Davenport, and V. Venturi. 2013. NKT and MAIT invariant TCRα sequences can be produced efficiently by VJ gene recombination. *Immunobiology.* 218:213–224. http://dx.doi.org/10.1016/j.imbio.2012.04.003

Haney, D., M.F. Quigley, T.E. Asher, D.R. Ambrozak, E. Gostick, D.A. Price, D.C. Douek, and M.R. Betts. 2011. Isolation of viable antigen-specific CD8+ T cells based on membrane-bound tumor necrosis factor (TNF)-α expression. *J. Immunol. Methods.* 369:33–41. http://dx.doi.org/10.1016/j.jim.2011.04.003

Kjer-Nielsen, L., O. Patel, A.J. Corbett, J. Le Nours, B. Meehan, L. Liu, M. Bhati, Z. Chen, L. Kostenko, R. Reantragoon, et al. 2012. MR1 presents microbial vitamin B metabolites to MAIT cells. *Nature.* 491:717–723.

Larkin, M.A., G. Blackshields, N.P. Brown, R. Chenna, P.A. McGettigan, H. McWilliam, F. Valentin, I.M. Wallace, A. Wilm, R. Lopez, et al. 2007. Clustal W and Clustal X version 2.0. *Bioinformatics.* 23:2947–2948. http://dx.doi.org/10.1093/bioinformatics/btm404

Le Bourhis, L., E. Martin, I. Péguillet, A. Guihot, N. Froux, M. Coré, E. Lévy, M. Dusseaux, V. Meyssonnier, V. Premel, et al. 2010. Antimicrobial activity of mucosal-associated invariant T cells. *Nat. Immunol.* 11:701–708. (published erratum appears in *Nat. Immunol.* 2010. 11:969) http://dx.doi.org/10.1038/ni.1890

Lefranc, M.P., C. Pommié, M. Ruiz, V. Giudicelli, E. Foulquier, L. Truong, V. Thouvenin-Contet, and G. Lefranc. 2003. IMGT unique numbering for immunoglobulin and T cell variable domains and Ig superfamily V-like domains. *Dev. Comp. Immunol.* 27:55–77. http://dx.doi.org/10.1016/S0145-305X(02)00039-3

López-Sagaseta, J., C.L. Dulberger, J.E. Crooks, C.D. Parks, A.M. Luoma, A. McFedries, I. Van Rhijn, A. Saghatelian, and E.J. Adams. 2013a. The molecular basis for Mucosal-Associated Invariant T cell recognition of MR1 proteins. *Proc. Natl. Acad. Sci. USA.* 110:E1771–E1778. http://dx.doi.org/10.1073/pnas.1222678110

López-Sagaseta, J., C.L. Dulberger, A. McFedries, M. Cushman, A. Saghatelian, and E.J. Adams. 2013b. MAIT recognition of a stimulatory bacterial antigen bound to MR1. *J. Immunol.* 191:5268–5277. http://dx.doi.org/10.4049/jimmunol.1301958

Martin, E., E. Treiner, L. Duban, L. Guerri, H. Laude, C. Toly, V. Premel, A. Devys, I.C. Moura, F. Tilloy, et al. 2009. Stepwise development of MAIT cells in mouse and human. *PLoS Biol.* 7:e54. http://dx.doi.org/10.1371/journal.pbio.1000054

Meierovics, A., W.J. Yankelevich, and S.C. Cowley. 2013. MAIT cells are critical for optimal mucosal immune responses during in vivo pulmonary bacterial infection. *Proc. Natl. Acad. Sci. USA.* 110:E3119–E3128. http://dx.doi.org/10.1073/pnas.1302799110

Patel, O., L. Kjer-Nielsen, J. Le Nours, S.B. Eckle, R. Birkinshaw, T. Beddoe, A.J. Corbett, L. Liu, J.J. Miles, B. Meehan, et al. 2013. Recognition of vitamin B metabolites by mucosal-associated invariant T cells. *Nat. Commun.* 4:2142. http://dx.doi.org/10.1038/ncomms3142

Porcelli, S., C.E. Yockey, M.B. Brenner, and S.P. Balk. 1993. Analysis of T cell antigen receptor (TCR) expression by human peripheral blood CD4−8− α/β T cells demonstrates preferential use of several Vβ genes and an invariant TCR α chain. *J. Exp. Med.* 178:1–16. http://dx.doi.org/10.1084/jem.178.1.1

Price, D.A., J.M. Brenchley, L.E. Ruff, M.R. Betts, B.J. Hill, M. Roederer, R.A. Koup, S.A. Migueles, E. Gostick, L. Wooldridge, et al. 2005. Avidity for antigen shapes clonal dominance in CD8+ T cell populations specific for persistent DNA viruses. *J. Exp. Med.* 202:1349–1361. http://dx.doi.org/10.1084/jem.20051357

Quigley, M.F., J.R. Almeida, D.A. Price, and D.C. Douek. 2011. Unbiased molecular analysis of T cell receptor expression using template-switch anchored RT-PCR. *Curr. Protoc. Immunol.* Chapter 10:Unit 10.33.

Reantragoon, R., L. Kjer-Nielsen, O. Patel, Z. Chen, P.T. Illing, M. Bhati, L. Kostenko, M. Bharadwaj, B. Meehan, T.H. Hansen, et al. 2012. Structural insight into MR1-mediated recognition of the mucosal associated invariant T cell receptor. *J. Exp. Med.* 209:761–774. http://dx.doi.org/10.1084/jem.20112095

Reantragoon, R., A.J. Corbett, I.G. Sakala, N.A. Gherardin, J.B. Furness, Z. Chen, S.B. Eckle, A.P. Uldrich, R.W. Birkinshaw, O. Patel, et al. 2013. Antigen-loaded MR1 tetramers define T cell receptor heterogeneity in mucosal-associated invariant T cells. *J. Exp. Med.* 210:2305–2320. http://dx.doi.org/10.1084/jem.20130958

Shen, W.-J., H.-S. Wong, Q.-W. Xiao, X. Guo, and S. Smale. 2012. Towards a mathematical foundation of immunology and amino acid chains. Available at: http://adsabs.harvard.edu/cgi-bin/bib_query?arXiv:1205.6031 (accessed February 17, 2014).

Thomsen, M.C., and M. Nielsen. 2012. *Seq2Logo*: a method for construction and visualization of amino acid binding motifs and sequence profiles including sequence weighting, pseudo counts and two-sided representation of amino acid enrichment and depletion. *Nucleic Acids Res.* 40:W281–W287. http://dx.doi.org/10.1093/nar/gks469

Tilloy, F., E. Treiner, S.H. Park, C. Garcia, F. Lemonnier, H. de la Salle, A. Bendelac, M. Bonneville, and O. Lantz. 1999. An invariant T cell receptor α chain defines a novel TAP-independent major histocompatibility complex class Ib–restricted α/β T cell subpopulation in mammals. *J. Exp. Med.* 189:1907–1921. http://dx.doi.org/10.1084/jem.189.12.1907

Treiner, E., L. Duban, I.C. Moura, T. Hansen, S. Gilfillan, and O. Lantz. 2005. Mucosal-associated invariant T (MAIT) cells: an evolutionarily conserved T cell subset. *Microbes Infect.* 7:552–559. http://dx.doi.org/10.1016/j.micinf.2004.12.013

Venturi, V., K. Kedzierska, S.J. Turner, P.C. Doherty, and M.P. Davenport. 2007. Methods for comparing the diversity of samples of the T cell receptor repertoire. *J. Immunol. Methods.* 321:182–195. http://dx.doi.org/10.1016/j.jim.2007.01.019

Young, M.H., L. U'Ren, S. Huang, T. Mallevaey, J. Scott-Browne, F. Crawford, O. Lantz, T.H. Hansen, J. Kappler, P. Marrack, and L. Gapin. 2013. MAIT cell recognition of MR1 on bacterially infected and uninfected cells. *PLoS ONE.* 8:e53789. http://dx.doi.org/10.1371/journal.pone.0053789